CHAPTER 11 [UNCORRECTED PROOF]

Rationale for Tau-Aggregation Inhibitor Therapy in Alzheimer's Disease and Other Tauopathies

CLAUDE M. WISCHIK,[1] DAMON J. WISCHIK,[2] JOHN M.D. STOREY[3] AND CHARLES R. HARRINGTON[1]

[1] TauRx Therapeutics Ltd. and School of Medicine and Dentistry, University of Aberdeen, Foresterhill, Aberdeen, AB25 2ZD, Scotland, UK; [2] Department of Computer Science, University College, Gower Street, London, WC1E 6BT, UK; [3] TauRx Therapeutics Ltd. and Department of Chemistry, University of Aberdeen, Meston Walk, Aberdeen, AB24 3UE, Scotland, UK

11.1 The Tau-Aggregation Pathology of Alzheimer's Disease

Alzheimer's disease (AD) is an irreversible, neurodegenerative disorder characterised by the progressive loss of memory and thinking skills. It was first presented at a meeting in 1906 by Dr. Alois Alzheimer, a German psychiatrist, who discovered "neurofibrillary tangles" in the brain tissue of a woman who died with dementia at the age of 55.[1] It was not until the tangle could be isolated and purified that its structure[2–4] and composition could be determined.[5,6] The neurofibrillary tangles are composed predominantly of tau protein, a protein essential for neuronal shape and axonal transport and the aggregation of tau is closely linked both to clinical dementia and cell death.[7–9] These findings have also been affirmed by others in the field.[10–14]

RSC Drug Discovery Series No. 2
Emerging Drugs and Targets for Alzheimer's Disease
Volume 1: Beta-Amyloid, Tau Protein and Glucose Metabolism
Edited by Ana Martinez

Published by the Royal Society of Chemistry, www.rsc.org

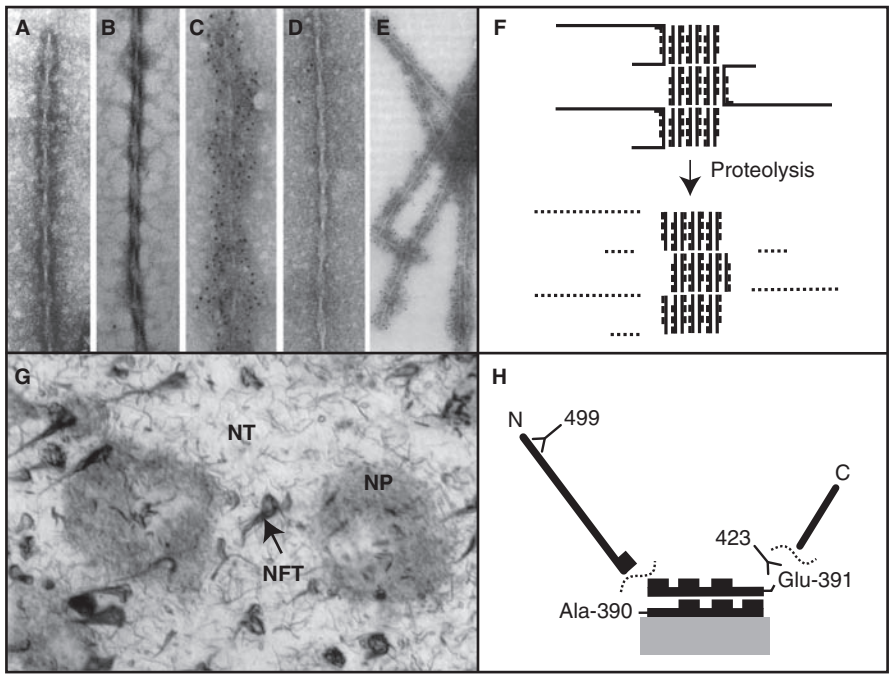

Figure 11.1 Neurofibrillary pathology is composed of aggregated tau in filaments. The filaments have a fuzzy coat (A) that can be removed by proteolysis (B). Immunolabelling shows that the fuzzy coat contains N-terminal parts of tau (C) that are removed by proteolysis (D), while the remaining PHF core contains fragments truncated at Glu-391 and recognised by mAb 423 (E). mAb 423 immunoreactivity can be demonstrated in PHFs and in intracellular pretangle tau oligomers without prior treatment with proteases and this is represented schematically (F). All neurofibrillary pathology is visualised in AD brain tissue using mAb 423 (NFT, neurofibrillary tangle; NT, neuropil threads; NP, neuritic plaque) (G). The process of aggregation has been simulated in an *in vitro* assay, using antibodies specific to the N-terminus (499) and C-terminal truncation of tau (423); dotted lines indicate sites of proteolytic cleavage (H).

Neurofibrillary tangles are intraneuronal clusters of aberrant tau protein polymers that consist of ''paired helical filaments'' (PHFs), thus termed from their characteristic double-twisted ribbon shape. The neurofibrillary tangle and its constituent PHFs are shown in Figure 11.1. PHFs have a fuzzy outer coat accounting for about 20% of the mass of the filament that can be removed by digestion with proteases leaving behind a stable inner core (Figures 11.1A–D) which retains the characteristic twisted ribbon structure. A monoclonal antibody (mAb 423), raised against core-PHFs, labels both isolated core filaments and intact PHFs (Figure 11.1E). Further research led to the discovery that the molecular configuration recognised by this monoclonal had been created in the brain by a series of events depicted in Figure 11.1F.[15] The short tau fragment of

which the core-PHF is principally composed creates the monoclonal antibody recognition site by means of a high-affinity binding and digestion process, leading to a specific C-terminal truncation at position Glu-391 in the tau molecule recognised by mAb 423. Thus, the entire spectrum of the tau-aggregation pathology seen in a histological section of the AD brain (Figure 11.1G) bears the hallmark of this aggregation/truncation process that can be modelled in the test tube (Figures 11.1F and A). This process underlies the tau-aggregation cascade described further in Section 11.2.

The image in Figure 11.1G serves to illustrate very clearly a simple fact that has often been lost sight of within the dominant β-amyloid theory, namely the sheer extent of the tau-aggregation pathology that is characteristic of AD. AD is the most common in a family of neurodegenerative disease characterised by prominent aggregation of tau protein, generally termed "tauopathies" (Figure 11.2).

The tauopathy of AD follows a highly characteristic pattern of spread of tau-aggregation pathology, illustrated in Figure 11.3. The characteristic overall distribution of neurofibrillary tangle pathology in the human brain in AD is shown in Figure 11.3A. It is most severe where it begins in the hippocampus and entorhinal cortex (ERC). As the disease progresses, tangles spread to the temporal, parietal and frontal cortices. This characteristic distribution of the tau-aggregation pathology seen postmortem closely matches the pattern of defects that can be demonstrated by functional brain scans during life. These scans reveal patterns of reduced neuronal function, either by way of reduced blood flow (HMPAO-SPECT) or reduced glucose utilisation (FDG-PET). As

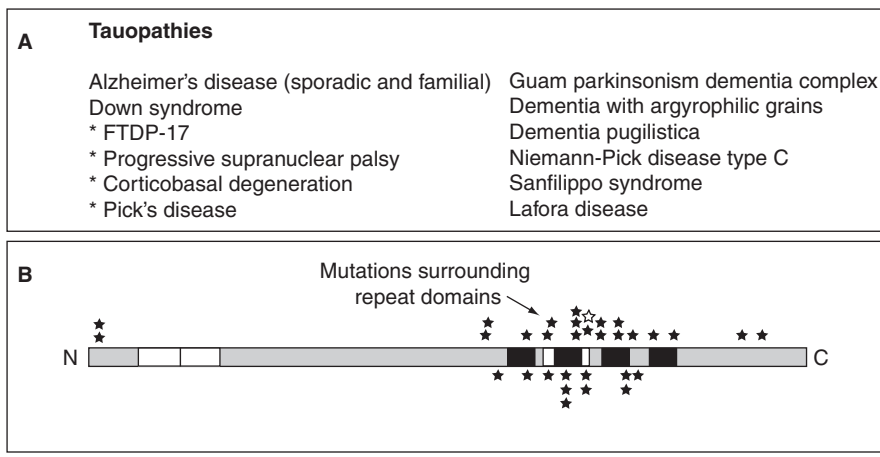

Figure 11.2 The tauopathies are neurodegenerative diseases characterised by tau-aggregation pathology (A). Those denoted with an asterisk have cases directly linked to mutations in the tau-protein gene. These mutations are typically clustered around the same repeat domains (B) found in the core-PHF structure (see Figures 11.1 and 11.7). Nearly 40 mutations have been identified, including 7 intronic mutations (open asterisk) that affect alternative splicing of exon 10 within the repeat domains.

shown in Figure 11.3B, there is progressive deterioration in neuronal function in the regions of progressive accumulation of aggregated tau. These scan deficits match the clinical progression of AD as measured by the mini-mental state examination (MMSE).[16,17]

This stereotyped pattern of spread of pathology has been formalised into the Braak staging system,[18] illustrated in Figure 11.3C. By taking a single brain slice through the brain region shown by the vertical line in Figure 11.3A, the spread of tau aggregation can be staged on the basis of microscopic examination of the brain into the six Braak stages illustrated in Figure 11.3C. It should be noted that Braak attempted to devise a staging system based on the β-amyloid pathology of AD, but showed that this was not possible because it appears to be a general feature of the aging brain, and does not appear to follow any clear pattern of progression or spread. It has since been confirmed by numerous studies that there is minimal if any systematic relationship between β-amyloid pathology and cognitive decline.[19–22]

Braak staging therefore provides a useful unifying schema for bringing together all of the key processes that characterise the evolution of AD from its earliest detectable stages through to end-stage dementia. This is shown in Figure 11.4. Figure 11.3B shows the approximate relationship between Braak stages and the defects shown by HMPAO-SPECT scan.[16] In Figure 11.4A, the relationship between Braak stage and decline in MMSE score is shown.[8] This data comes from a prospective clinicopathological study conducted in an epidemiologically defined cohort in the Cambridge area in which patients were followed in the community by means of repeat assessment every 12–24 months. Because cases were followed irrespective of disease severity or diagnosis, it became possible to establish a calibration between level of cognitive function and Braak stage, once cases with vascular pathology were excluded. What is striking in Figure 11.3B is that already at preclinical and early clinical stages of AD, brain pathology has already advanced to Braak stages 2 and 3. The transition to Braak stage 4 corresponds to disease severity generally meeting agreed clinical criteria for a diagnosis of AD.

The process of tau aggregation begins in the neocortical regions well before neurofibrillary tangles appear (Figure 11.4). Tau aggregation, in the form of proteolytically stable PHFs, can be detected from Braak stage 2 onwards. Tangles that can be visualised by conventional microscopy do not appear until Braak stage 4 in the neocortex. As will be shown below, the time interval between Braak stages 2 and 4 is about 20 years. There is therefore a long pretangle/preclinical and early clinical period during which therapeutic intervention in the tau-aggregation cascade can be achieved.

Tau aggregation begins in the form of submicroscopic formations referred to as tau oligomers (Figure 11.5). This progress to filaments (*i.e.* PHFs) that, when they occupy the whole of the intracellular space, are referred to as a neurofibrillary tangle ("NFT"). This eventually chokes the neurone by eliminating the possibility of normal neuronal metabolism and in the process eventually leaves behind an extracellular "ghost" tangle as the only marker of a previously existing neurone.

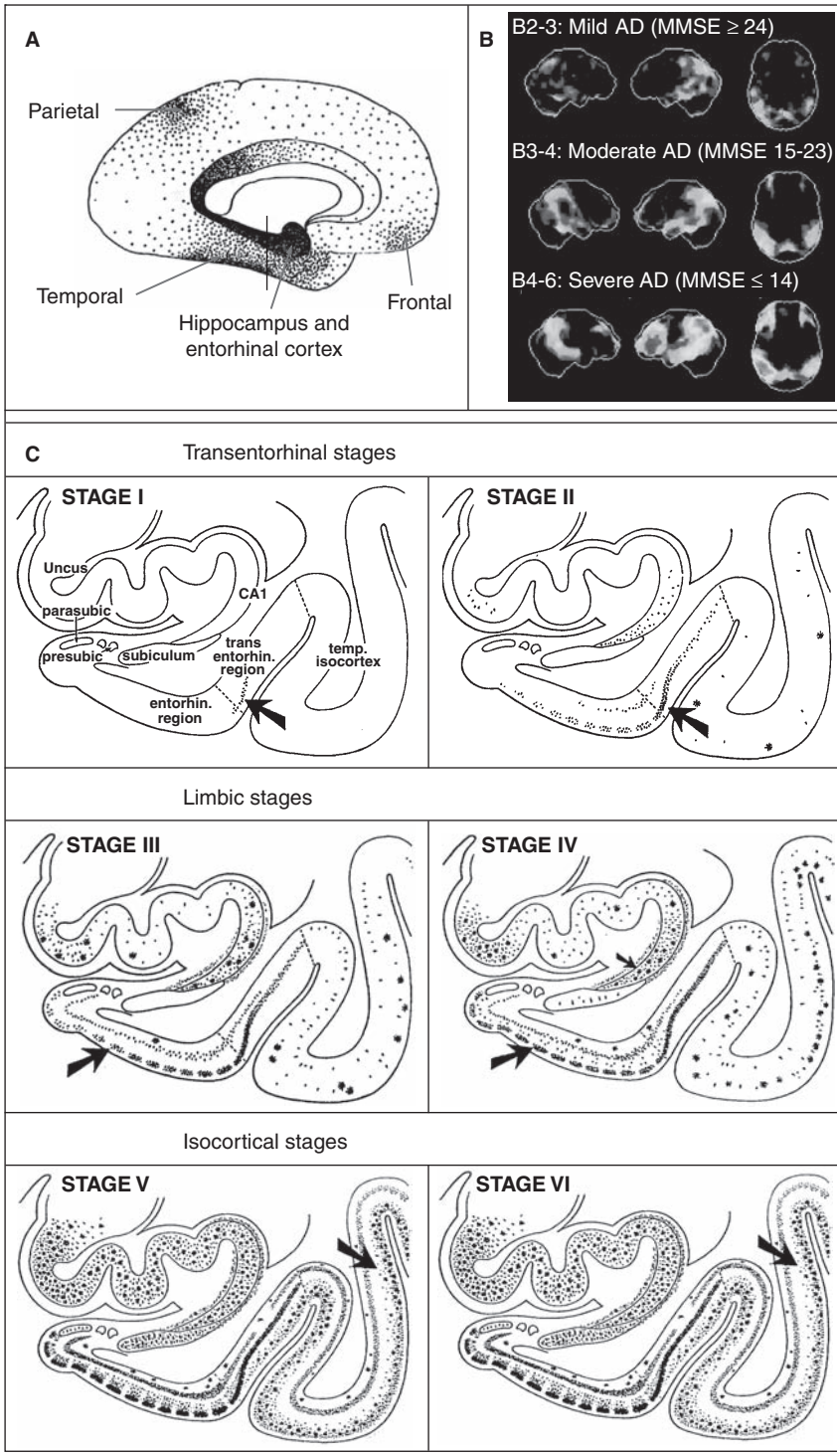
A
Parietal
Temporal
Frontal
Hippocampus and
entorhinal cortex
B
B2-3: Mild AD (MMSE ≥ 24)
B3-4: Moderate AD (MMSE 15-23)
B4-6: Severe AD (MMSE ≤ 14)
C
Transentorhinal stages
STAGE I
Uncus
parasubic
presubic
subiculum
CA1
trans
entorhin.
region
temp.
isocortex
entorhin.
region
STAGE II
Limbic stages
STAGE III
STAGE IV
Isocortical stages
STAGE V
STAGE VI

The progressive accumulation of ghost tangles also follows Braak stages. Tangle-mediated cell death begins in the entorhinal cortex at Braak stage 2 and progresses thereafter. Destruction of neurones in the hippocampus begins at around Braak stage 3 and likewise progresses at a lower rate. Finally, tangle-mediated neuronal destruction does not become apparent in the neocortical regions (frontal, temporal and parietal neocortex) until Braak stage 5.

These figures illustrate that the whole process of tau-aggregation pathology follows an impressive and very clearly defined sequence, from the earliest stages when tau oligomers and filaments begin to form, through to the final stages when neurones are killed by the mature neurofibrillary tangles. All of these processes at the pathological level map to clinically measurable stages of cognitive deficit and physically to stages of loss of brain function that can be measured by currently available brain-scanning techniques.

Braak staging can also be mapped throughout the human lifespan. In a major study, Braak's group reported the results of one of the largest human postmortem studies ever conducted in 847 cases in whom age and Braak stage were reported between ages 45–95.[23] There were approximately 17 cases per year of life throughout this age span. A Kaplan–Meier survival analysis using this data is shown in Figure 11.6. The probability of transition from one stage to a later stage demonstrates that there is a simple age-dependent transition to higher Braak stages with advancing age (Figure 11.6A). This indicates that, irrespective of the claims of the β-amyloid theory regarding specific genetic causation of AD, the entire process is clearly embedded within the blueprint of the general aging human population and regardless of specific genetic factors that may accelerate the process in some individuals.

The survival plot can be transformed into a prevalence plot at specific Braak stages. This gives a cross-sectional view of population progression by age through the Braak stages through the ages 40–95. The peak for Braak stage 1 is around 50 years. Considering the population aged 65 and over, only 24% will remain at Braak stage 0 for the remainder of their lives. Of the 41% of the population who progress to Braak stage 2, which peaks at around age 65, 92% will progress to Braak stage 3, which peaks at around age 75. Progression to Braak stage 4 is limited by the reduction in survival population beyond age 75. The most surprising conclusion to be drawn from Figure 11.6B is that Braak stage 2, which appears clinically innocuous from Figure 11.4 (*i.e.* corresponds to the maximum MMSE score of 30), is actually already on what appears to be a largely irreversible pathway of future inexorable disease progression. This analysis is fundamentally at odds with the claims made by the β-amyloid school

Figure 11.3 Braak staging of Alzheimer's disease. Tau aggregation spreads in a characteristic neuroanatomical pattern (A) and the distribution of tau pathology matches the pattern of SPECT scan defects seen in early stages of AD (B). (C) The Braak staging of the spread of tangles from medial temporal lobe to neocortex can be assessed in a single brain slice (C). [B from Nishimura *et al.* 2007[16] and C from Braak and Braak, 1991;[18] with permissions].

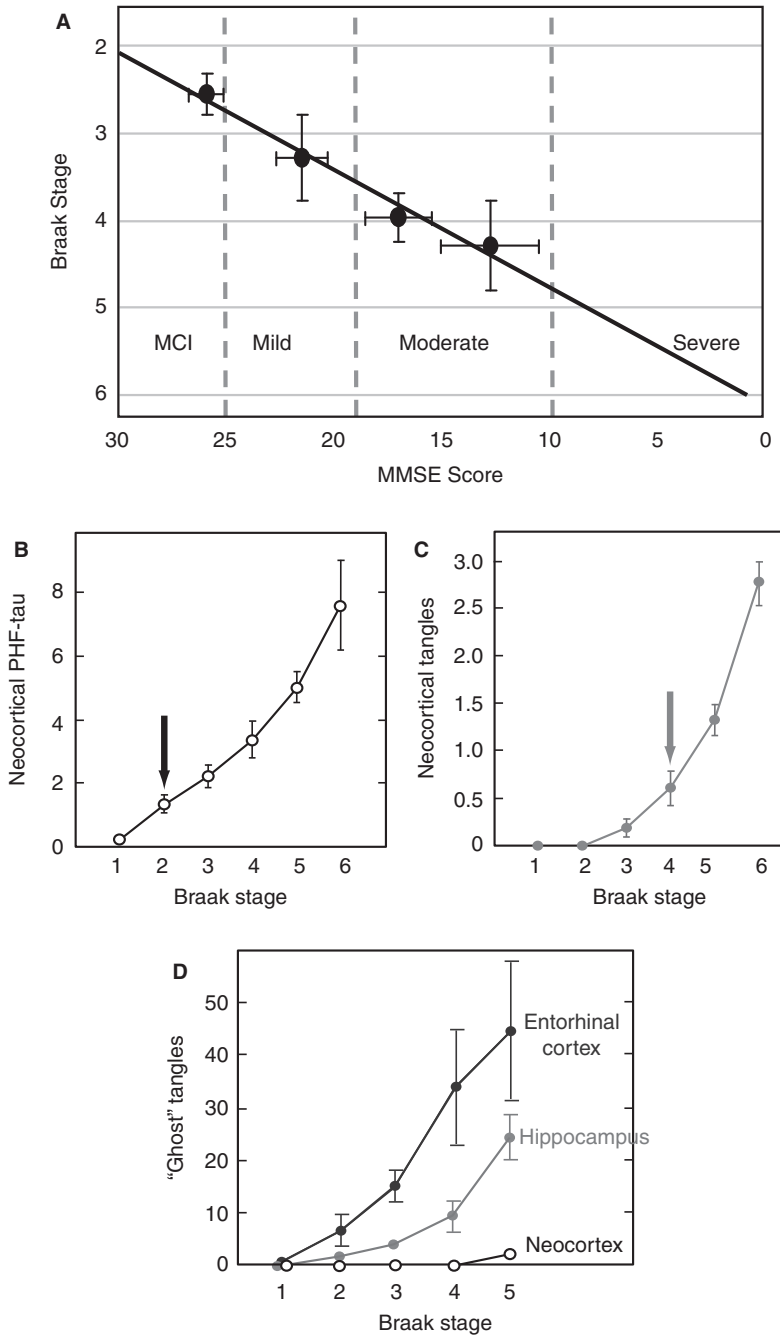

Figure 11.4 Braak staging measures cognitive decline (A), tau aggregation (B), neurofibrillary tangle pathology (C) and tangle-mediated neuronal destruction (D). Results from a prospective clinicopathological study.[7,8]

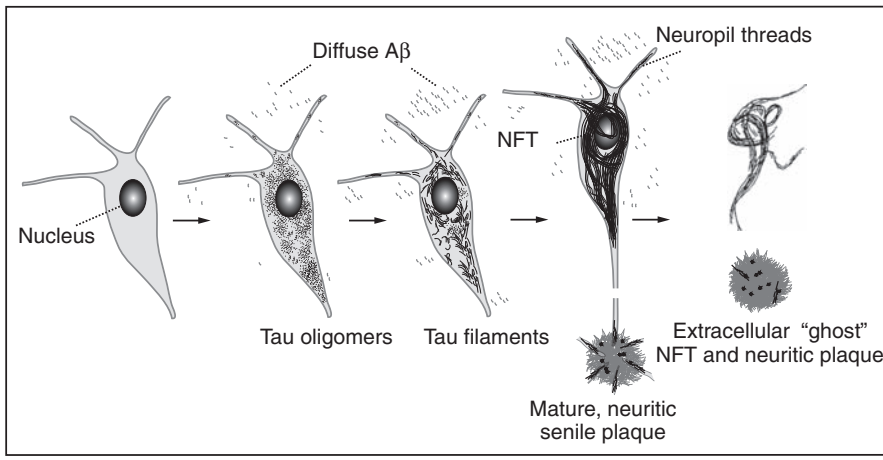

Figure 11.5 Development of tau pathology initiates with the deposition of Tau, first as oligomeric species that then progress to filaments. These PHFs accumulate and develop into the NFTs. Defective axonal transport affects the transport of APP to synapses and its recycling in the opposite direction, thus leading to an accumulation of Aβ in the form of the mature, neuritic senile plaque. This, together with PHF-tau from other neurites, constitutes the neuritic senile plaque. Finally, the extracellular "ghost" tangle remains as a vestige of the neuron that has been destroyed.

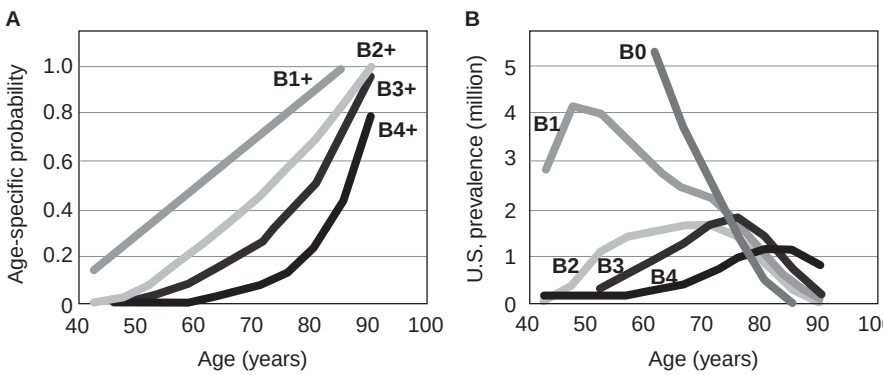

Figure 11.6 The epidemiological implications of Braak staging with respect to age. (A) Age-specific probability of Braak stage transitions calculated from the data derived from 847 postmortems.[3] (B) Estimated prevalence of different Braak stages by age for the US population.

of thought, to the effect that tau-aggregation pathology is a late-stage event and therefore not amenable to therapeutic intervention. On the contrary, the real challenge facing the field is to identify those individuals at Braak stage 2 in whom prevention of the further progression of pathology could essentially eliminate AD from the aging human blueprint.

11.2 The Molecular Mechanics of Tau Aggregation in Alzheimer's Disease

As indicated above, PHFs which come from intracellular tangles are associated with a fuzzy outer coat that can be removed by proteolysis, which reveals the twisted ribbon structure of the core-PHF. What is more important to understand is that removal of the fuzzy coat removes all of the phosphorylated tau immunoreactivity that is present in PHFs, and that this does not affect the structural stability of the filament. The only tau-protein fragment present within the core of the PHF is a short fragment of only about 100 amino acid residues in length that comes from the repeat-domain of tau. That is, it represents less than a quarter of the full-length tau molecule. How this fragment comes into existence in the brain and why it should be found as the fundamental building block of the core-PHF came from studies that showed that the core-tau unit of the core-PHF has the remarkable property that it is able to reproduce itself at the expense of normal tau.[8]

The core fragment of tau attached to a solid-phase permits a high-affinity binding interaction with full-length tau (Figure 11.7A). This locks the repeat domain of the bound full-length molecule into a proteolytically stable configuration that is essentially identical to the starting fragment. That is, the digestion step with a broad spectrum exoprotease recreates the core-tau fragment. Digestion removes the other parts of the molecule, but fails to remove the bound segment that constitutes the new replicate of the original core-tau template. The fundamental problem is that the proteolytically stable aggregate retains the ability to bind yet more normal tau protein through subsequent binding/digestion cycles. This process creates the mAb 423 antibody recognition site already alluded to in Figure 11.1, and shown to be such a prominent feature of the AD tauopathy.

The process shown schematically in a cell-free environment (Figure 11.7A) was also confirmed in a cellular environment in the form of a stable cell line suitable for screening of tau-aggregation inhibitors (Figure 11.7B).[24] In this cell line, expression of normal full-length tau is under the control of an inducer that can be turned on in the presence of IPTG (arrow-head). The cell line also has very low level constitutive expression of the core-tau PHF unit (thick arrow). The levels of the latter have to be extremely low, otherwise toxic aggregates are readily formed. When tau expression is turned on, by the addition of IPTG, there is a conversion of the full-length tau into the truncated core-tau PHF unit. This induction is associated with the appearance of tau protein aggregates that are recognised by a proprietary, fluorescent aggregation-dependent ligand (Figures 11.7C and D). Simple overexpression of full-length tau does not lead to aggregation in this model.

The capacity of tau-protein pathology to propagate itself at the expense of normal tau was confirmed in recent independent studies. Aggregated fibrils of tau243-375 can be taken up into cells *in vitro* containing full-length tau and passed on to neighbouring cells to seed aggregation.[25] Similarly, the

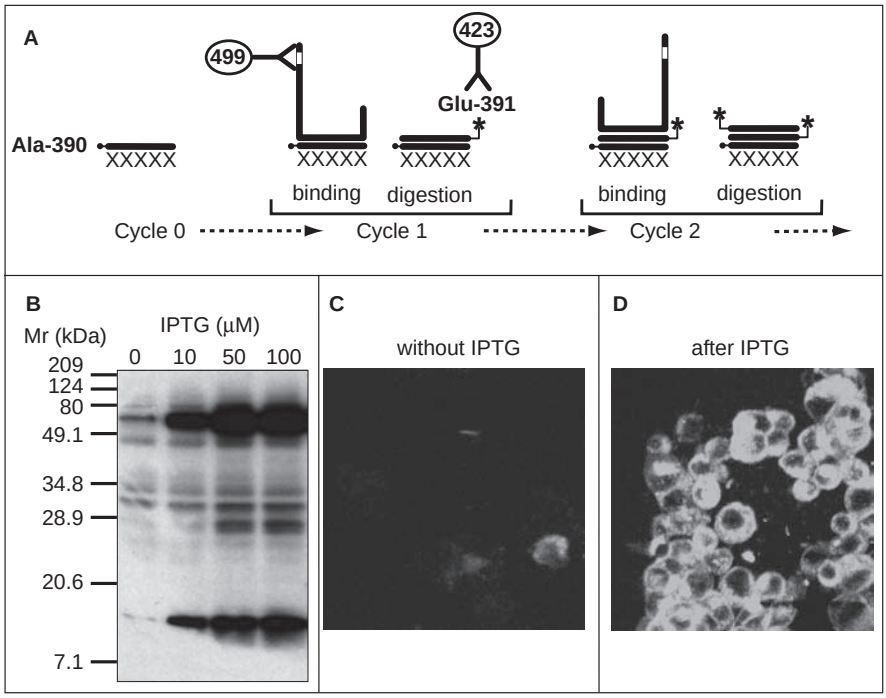

Figure 11.7 The core-PHF is composed of truncated tau protein that aggregates via an autocatalytic process of binding and proteolysis, depicted schematically (A). In a cellular model (B), induction of expression of full-length tau (arrowhead) leads to the accumulation of 12-kDa truncated tau (arrow) in cells constitutively expressing low levels of truncated tau that serves as a seed for tau capture and propagation. Cells are labelled by a fluorescent PHF-ligand only after induction (C) and not in the absence of IPTG (D).

transmission and spread of tau pathology from tau-mutant mice into normal mice was achieved, provided the latter already expressed human full-length tau protein.[26]

The place of tau-aggregation pathology and of Tau aggregation inhibitor therapy is illustrated schematically in Figure 11.8. In general, the critical event in triggering the tau-aggregation cascade is the nucleation or seeding event (Figure 11.8A). Once the seeding event has occurred, the tau-aggregation cascade is self-propagating, and leads to two deleterious outcomes. It converts normal functional tau protein into the truncated aggregated form found in PHFs. This leads to a loss of normal tau protein,[27] needed to stabilise axonal microtubules for linking different parts of the brain. More importantly, as alluded to above, the tau aggregates are directly neurotoxic and eventually lead to neuronal death.

Although the β-amyloid school of thought sets great store by the abnormal processing of APP and/or presenilin as a critical upstream trigger for the

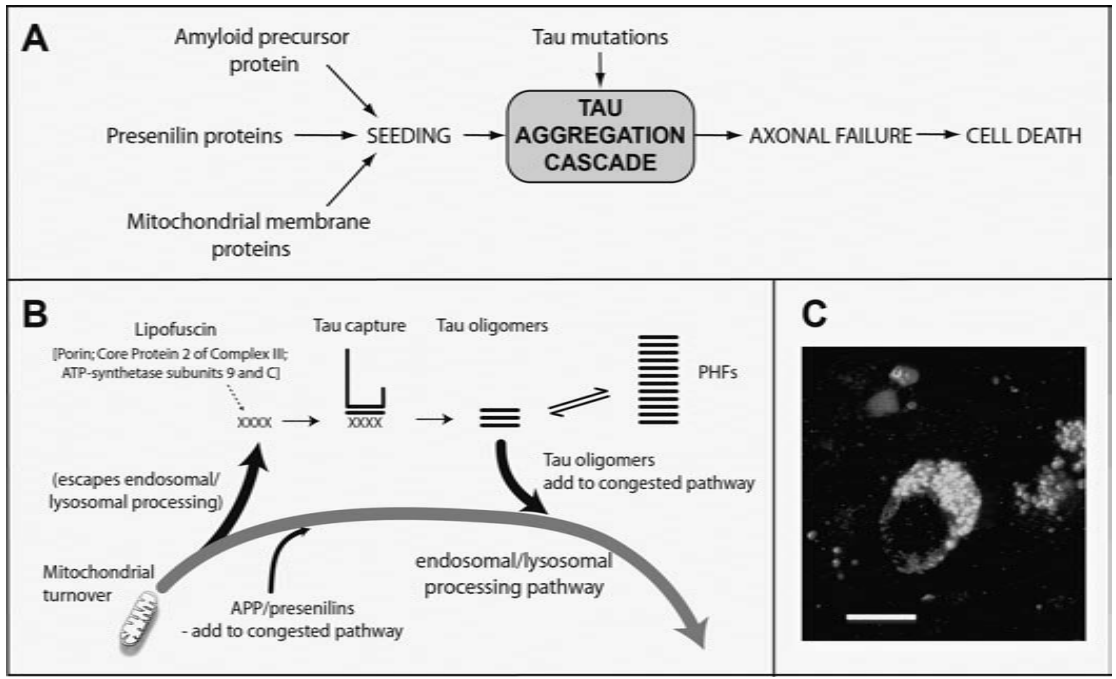

Figure 11.8 Tau aggregation is in a pivotal part of the degenerative process in AD and other tauopathies. (A) The initial seeding of tau protein may be initiated by any one or more events, *e.g.* mutations in APP, presenilin proteins, altered processing of mitochondrial membrane proteins or, more directly, through mutations in tau itself. (B) The aggregation of tau protein adds to the age-related congestion of the endosomal-lysosomal pathway. (C) The capture of tau by mitochondrial membrane proteins is illustrated in neurons in AD where there is colocalisation of tau and porin in lysosomes.

tau-aggregation cascade, a more general age-related abnormality in the endosomal-lysosomal processing pathway may be much more important, particularly the processing of mitochondria.[28] There are now two examples of tauopathies caused by genetically inherited abnormalities in the endosomal-lysosomal processing pathway: Niemann–Pick Type C[29] and Sanfilippo Syndrome Type B[30] entirely unrelated to any abnormality in APP processing.

In the case of sporadic AD, we consider that an age-related defect in the turnover of mitochondria is more important than APP.[28] This is illustrated in Figure 11.8B. Mitochondria are the obligate energy source for neuronal metabolism and their turnover period is approximately 6 months. Long-lived, nondividing cells such as neurones show signs of failure in the turnover of mitochondria-derived proteins as they age. These take the form of so-called aging pigments, or lipofuscin, which are in fact composed predominantly of unprocessed products of mitochondrial turnover.[31] These same proteins are found in close association with early-stage tau aggregates in the AD brain, and biochemical analyses show they have the ability to form resistant proteolytically stable complexes with tau. We have observed colocalisation of the mitochondrially derived proteins (porin, core protein 2 of complex III and ATP synthase subunit 9) with early tau aggregates. An example is shown for porin and tau (Figure 11.8C). Essentially identical images have been produced in Sanfilippo syndrome showing colocalisation of tau with lysozyme and a lysosomal form of ATP-synthase subunit C.[30]

The system whose failure is responsible for clearance of mitochondria-derived proteins is the endosomal-lysosomal processing pathway, and is exactly the same pathway required for processing mutant membrane-bound proteins, such as APP and the presenilin proteins.[32] Therefore, mutations in these proteins may add to the congestion and dysfunction in this pathway without actually being directly causative of AD.

Once tau aggregation has been initiated, the only pathway available for clearance of the tau oligomers is the same congested endosomal-lysosomal pathway. The capacity of the neuron to clear proteolytically stable tau oligomers is therefore critically compromised, leading to uncontrolled progression of the tau-aggregation process. The progressive rate of accumulation of aggregated tau in the form of PHFs is, in fact, exponential over time (Figure 11.9). This can be calculated on the basis of levels of aggregated tau protein measured in neocortex at different Braak stages (as shown for example in Figure 11.4B) and real time between Braak stages, calculated for example from the data shown in Figure 11.6A.[23] From this it is possible to deduce the level of aggregated tau in neocortex as a function of time in years (Figure 11.9).

The critical transition points such as conversion to Braak stages 2–4 and the appearance of clinically visible dementia occur about 7 years after the transition to the steep exponential phase of tau aggregation in neocortex (Figure 11.9, arrow). This occurs about 25 years after the transition to Braak stage 1.

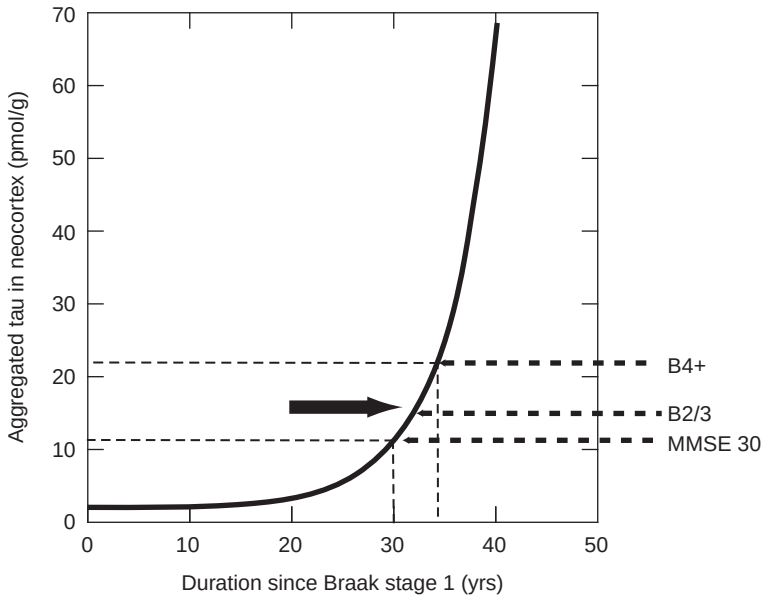

Figure 11.9 The exponential accumulation of aggregated tau in neocortex in humans calculated from a prospective clinicopathological study based on Braak staging. The arrow indicates stage at which clinically visible dementia is observed.

11.3 The Basis of Tau-Aggregation Inhibitor Therapy

Given the autocatalytic/self-propagating nature of the tau-aggregation cascade, it is possible to construct a mathematical model of a system that contains a self-propagating component (Figure 11.10A). In this model, normal tau protein is diverted into an aggregation cascade with a positive feedback component. There are two different timeframes operating in the data incorporated into the model. The times required for aggregation and clearance phenomena *in vitro* are relatively short (hours/days) whereas the time scale over which aggregates build up in the brain is measured in years, *i.e.* the time scale of Braak staging. Since production and clearance can be shown *in vitro* and in cell models to reach equilibrium over a short time (hours/days), the progressive slow build-up of aggregated tau over years cannot be explained by short-acting internal equilibrium processes. Rather, the progressive accumulation over time must be due to progressive failure of clearance that undergoes very gradual degradation. This is envisaged as a slow deterioration in the capacity of the endosomal-lysosomal system to deal with clearance of oligomers and larger tau aggregates. We have modelled this by incorporating the time required for the aggregation and dissolution processes observed *in vitro*, and an underlying long-term component that leads to decreased clearance capacity over time.

It then becomes possible to calculate the predicted consequences of intervention on the input side or enhancement on the clearance side (Figure 11.10A).

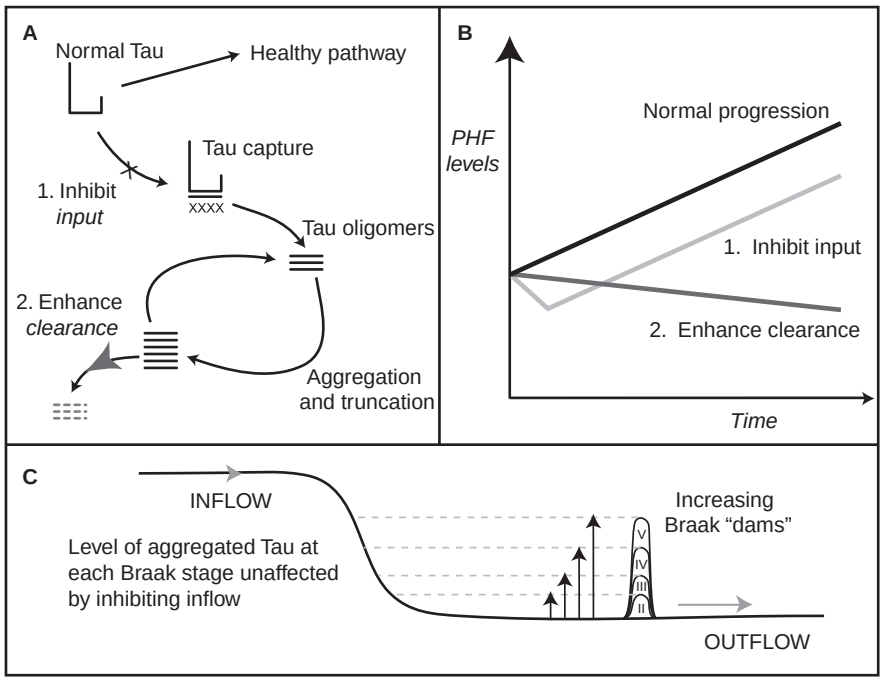

Figure 11.10 Opening up a new clearance pathway via tau disaggregation of oligomers via a tau-aggregation inhibitor (TAI) is the only way to affect the rate of disease progression. The tau-aggregation cascade proceeds by an autocatalytic process of binding and proteolysis of tau. (A) Braak progression is likely driven by age-related impairment in clearance of aggregated tau (*i.e.* progressive degradation of the endosomal-lysosomal pathway (see Figure 11.8B). (B) Only by enhancing clearance of oligomers by means of TAI treatment is the rate of progression of AD likely to be altered. (C) Inhibiting the inflow to the cycle will not affect the levels of aggregated tau accumulating at each Braak stage. Thus, upstream inhibition of factors that initiate tau capture are unlikely to alter the rate of progression of AD.

Although it seems intuitively obvious that inhibition on the input side should be beneficial, the model output indicates that the benefit of input-side intervention would be short lived (Figure 11.10B). The two axes represent time (in years) and corresponding PHF levels (*e.g.* in neocortex based on data such as that shown in Figure 11.9). The surprising conclusion is that a treatment that reduces the influx of tau into the aggregating cascade would be expected to have clinical characteristics of a purely symptomatic treatment. Despite input-side intervention appearing to act mechanistically on what might be postulated to be a rate-limiting aspect of the disease process, the net effect would be to produce only a transient reduction in levels of aggregated tau, but would have no effect on the long-term rate of accumulation of aggregated tau in the brain over time (Figure 11.10B). In other words, the intervention would be expected to produce

only transient benefit, and not impact on the subsequent rate of disease progression. On the other hand, an intervention on the output side of the process (*i.e.* enhanced clearance) would have the effect of altering the disease progression trajectory.

This appears somewhat counterintuitive but, but it is possible to explain in simpler terms what the mathematical model is showing (Figure 11.10C). One might envisage this as a system in which there is flow of water into and out of a dam. At equilibrium, input equals output, but input does not determine the level of water in the dam. The water level can be taken as analogous to the Braak stage, or level of aggregated tau in the brain. This is determined by the height of the barrier. Because inhibition on the input side could not conceivably achieve 100% efficacy, the effect of retarding input will produce a short-lived reduction that will again reach an equilibrium determined by the height of the barrier at a lower input/output equilibrium. The only way to avoid this, therefore, is to devise a treatment that lowers the level of the barrier.

The dynamics of this model apply irrespective of the biological mechanism that is postulated as being critical on the upstream side. This might be envisaged as tau hyperphosphorylation (despite the strictly biological arguments against the phosphorylation hypothesis of tau aggregation[28]) or some other putative upstream mechanism that might be mediated by APP. In short, the model predicts that upstream intervention in a process that has an autocatalytic component is essentially useless. Furthermore, it has been shown recently that tau-protein expression is actually required for Aβ-induced neuronal dysfunction and cognitive impairment in transgenic mice.[33]

11.4 Methylthioninium Chloride as a Tau-Aggregation Inhibitor

Methylthioninium chloride (MTC; Structure 11.1) was the first tau-aggregation inhibitor (TAI) reported[15] and the only TAI yet to be tested in clinical trials for AD.

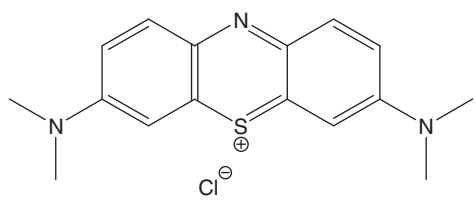

TAI therapy, such as that provided by MTC, acts essentially on the output side by enhancing clearance. The fundamental kinetic block in the clearance of aggregated tau is envisaged as being due to the state of aggregation itself. MTC was shown to reverse the proteolytic stability of the tau-protein fragment of the

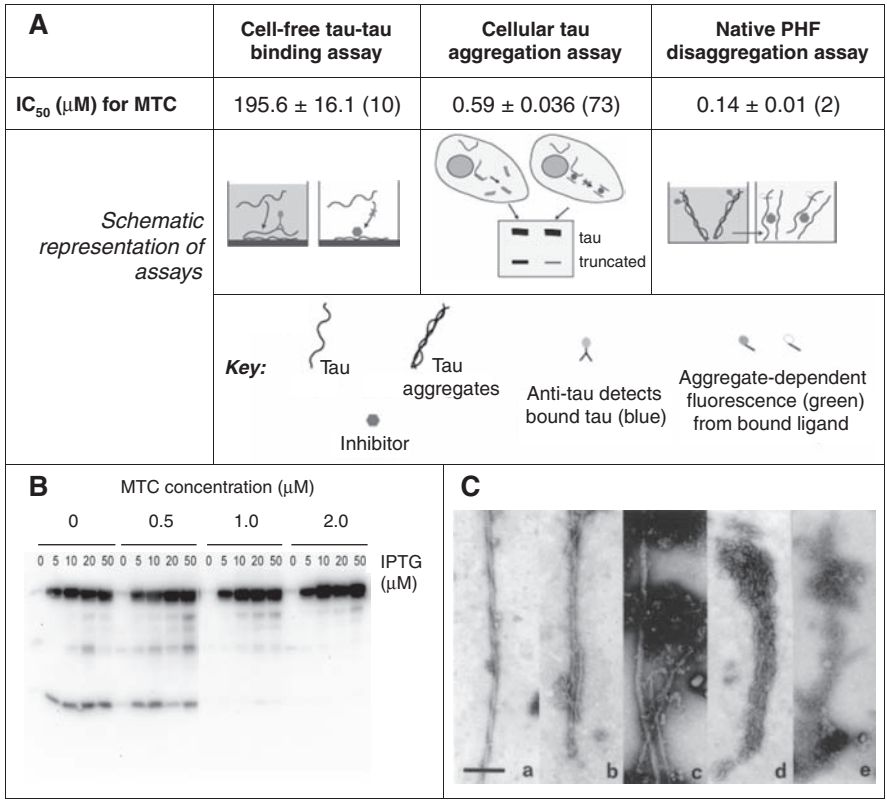

Figure 11.11 MTC is a tau-aggregation inhibitor that dissolves both oligomers and filaments. (A) Inhibitory activity of MTC in three assays shown diagrammatically. (B) Oligomeric tau produced in cells, as indicated by a 12-kDa fragment, is removed by MTC. (C) PHFs isolated from AD brain tissue are dissolved by increasing concentrations of MTC (a, 0.01%; b, 0.1% and c–e, 1%).

core-PHF by disaggregating the polymer, permitting the release of the core-tau monomer.[15] In its monomeric state, the core-tau unit of the PHF is extremely sensitive to proteases. PHFs disaggregate in the presence of MTC and MTC is effective at submicromolar concentrations in cell-free and cellular assays used to screen TAI activity (Figure 11.11).

The activity of MTC has been tested *in vivo* in two proprietary transgenic mouse models. In the first model, "Line 1" mice express the core-tau unit of the PHF linked with a short N-terminal signal-sequence and under the control of a neuron-specific Thy-1 promoter (Figure 11.12A).[34] The purpose of the signal sequence is to force tau aggregation by targetting expression to a system capable or providing an initiation binding substrate, *i.e.* the endoplasmic reticulum, and simultaneously forcing tau clearance into the endosomal-lysosomal pathway reproducing the conditions for a failure of this clearance pathway in

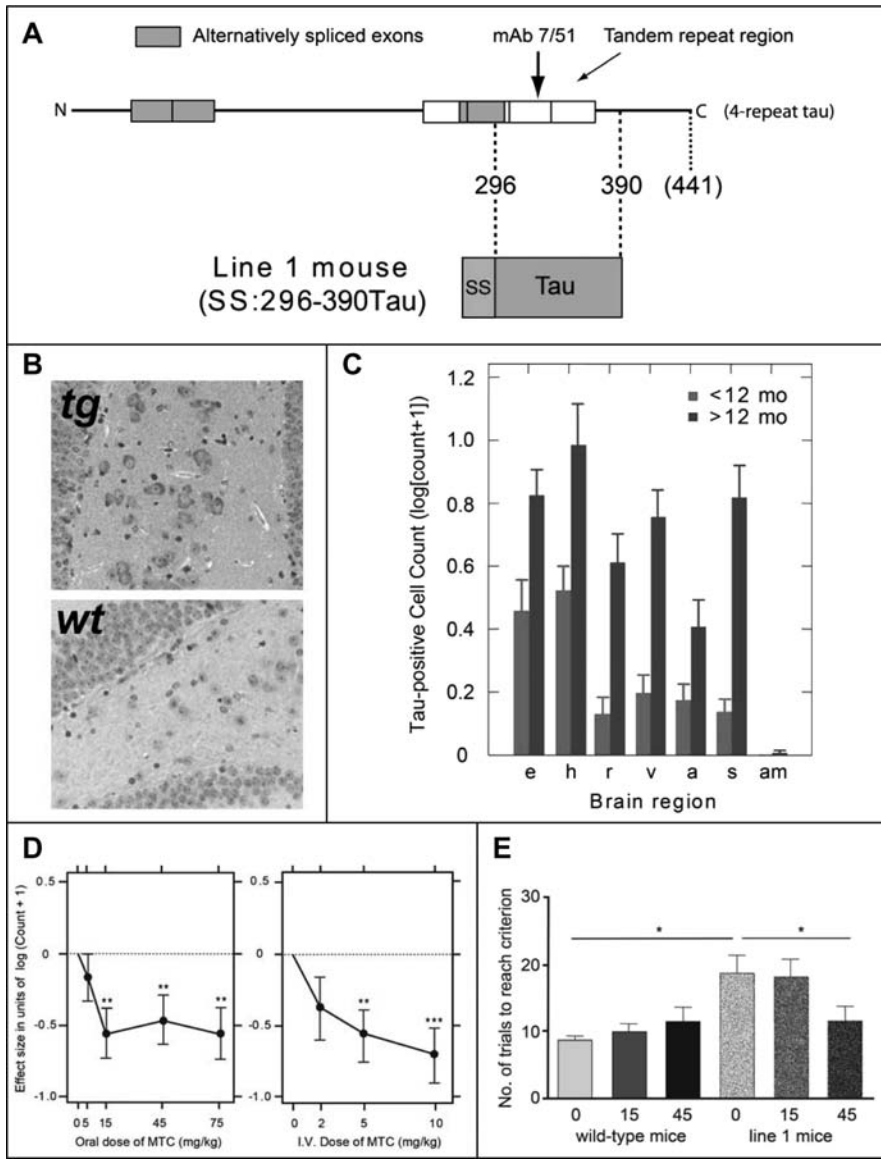

Figure 11.12 Line 1 mouse expresses truncated tau targeted to membrane via a signal sequence peptide (SS:296-390Tau; A). Pathology develops first in hippocampus and entorhinal cortex before progressing to other cortical areas (B, C). Pathology (D) and behavioural deficits in water maze learning (E) respond to treatment with MTC. (tg, transgenic; wt, wild type; e, entorhinal cortex; h, hippocampus; r, retrosplenial cortex; v, visual cortex; a, auditory cortex; s, subiculum; am, amygdala).

respect of tau. The net effect is to produce a pathology that reaches the stage of oligomers but not of fully formed filaments or neurofibrillary tangles (Figure 11.12B). The mice reproduce the essential phenomena of Braak staging (Figure 11.12C). In mice less than 12 months of age, the aggregated-tau pathology is located predominantly in the entorhinal cortex and hippocampus, but little in other brain regions. As mice age, the pathology spreads into isocortical brain regions (retrosplenial, visual and auditory cortices and subiculum). There is a reduction in the counts of tau-positive neurones containing oligomeric tau after mice have been treated with MTC (administered either orally or intravenously) (Figure 11.12D).

Line 1 mice develop a learning impairment after about 7 months of age, as shown for example in a modified Morris water maze,[35] in which the task is to find a hidden platform with a minimum number of trials. Line 1 mice require about twice as many trials to reach a given learning criterion and oral treatment with MTC reverses this learning defect (Figure 11.12E).

Truncated tau was directed to the endoplasmic reticulum in Line 1 mice to enable the initiation of tau nucleation and avoid the toxic effects observed by overexpressing truncated tau within cells. Mice expressing mutant tau exhibit increased tau associated with rough ER in motor neurons and a greater number of contacts between rough ER and mitochondria was observed.[36] Increased tau was also associated with a rough ER fraction extracted from AD brains compared with controls.

MTC also exhibits efficacy in a second proprietary mouse model (''Line 66''; Figure 11.13). In this case, a full-length tau construct with two mutations, at P301S (associated with frontotemporal dementia with Parkinsonism linked with chromosome 17, FTDP-17[37]), and a further mutation at G335D shown to further enhance tau aggregation *in vitro*. Whereas the Line 1 mouse exhibits diffuse neuronal tau pathology, the Line 66 mouse, has severe tau pathology, to an extent similar to that noted by other researchers expressing tau with FTDP-17 mutations in transgenic mice.[38–40] Tau tangles that stain positively with Bielschowsky silver and with thioflavin S indicate their filamentous nature. Tau pathology is observed in CA1 and CA3 of the hippocampus, entorhinal and other cortical areas (Figure 11.13B).

Line 66 mice show a severe abnormality of motor learning whereby they are unable to learn how to remain on a rotating rod (Figure 11.13C). Following oral treatment with MTC (1 mg/kg), however, this learning deficit is reversed. Somewhat higher doses (10 mg/kg) are required to reverse tau pathology in hippocampus and entorhinal cortex (Figure 11.13D). It is possible to extract protease-resistant 12-kDa tau from brains of Line 66 mice, indicating the presence of AD-like filaments of tau. This protease-resistant tau can be dissolved in the presence of MTC (Figure 11.13E).

Thus, MTC is able to reverse both the behavioural and pathological effects that arise *in vivo* in two transgenic mouse models of tau aggregation: a cognitive phenotype model in which tau oligomers predominate (Line 1) and a frontotemporal-like motor phenotype in which abundant filamentous tau accumulates (Line 66).

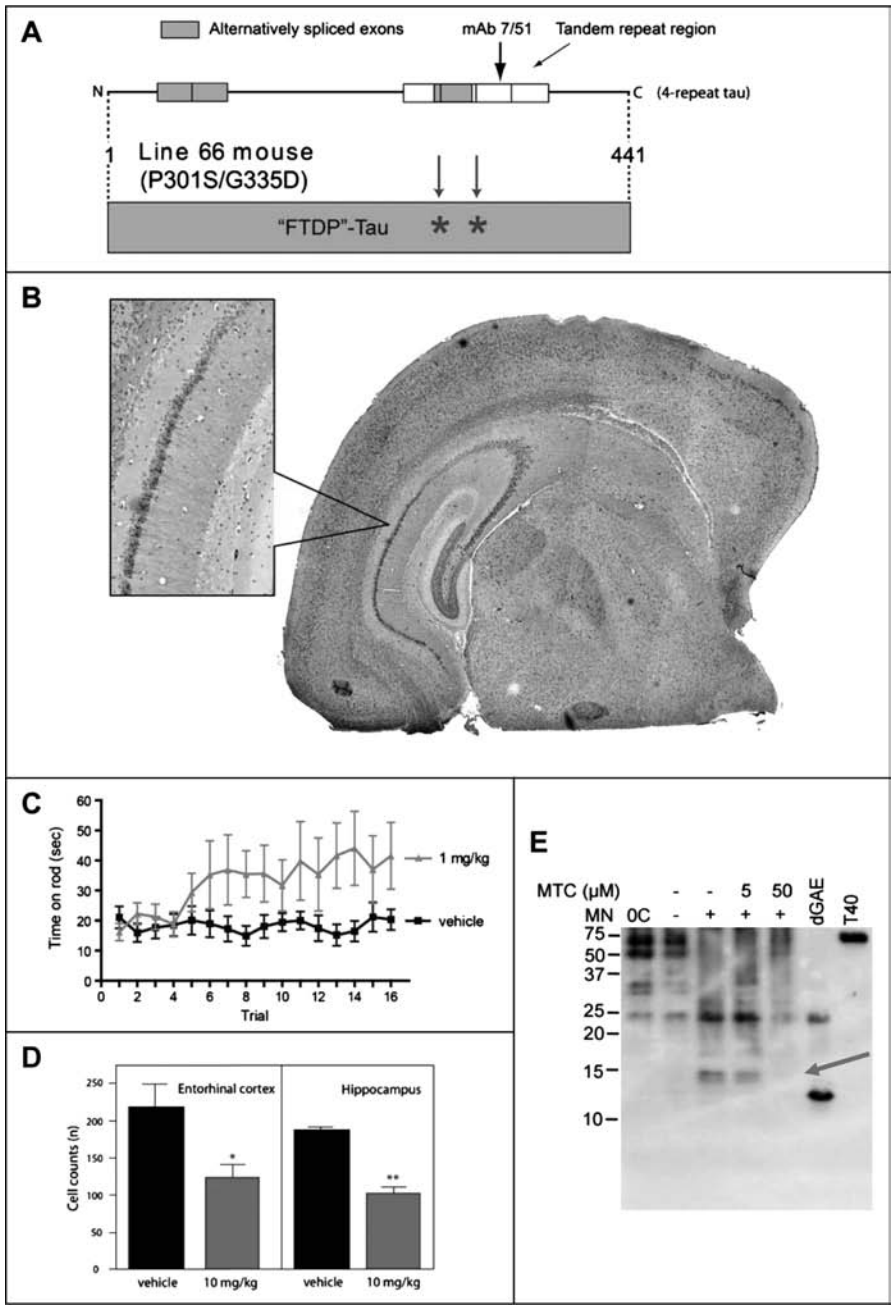

Figure 11.13 Transgenic ''FTDP-type'' tau mice (A) exhibit tau pathology throughout brain including hippocampus (B) and a motor phenotype. Both the pathology in entorhinal cortex and hippocampus (C) and motor learning on a Rotarod (D) are improved following oral treatment of Line 66 mice with MTC. Protease-resistant 12-kDa tau from brains is also sensitive to MTC (E, arrow).

11.5 Clinical Application of Tau-Aggregation Inhibitor Therapies

MTC was the first tau-aggregation inhibitor described,[15] and several other polymerisation inhibitors have since been reported. These include benzothiazole derivatives,[41,42] Congo red derivatives and anthraquinones,[43] 2,3-di(furan-2-yl)-quinoxalines,[44] phenylthiazolyl-hydrazide,[45] polyphenols and porphyrins,[46] cyanin dyes[47] and aminothienopyridazines.[48]

Importantly, MTC selectively avoids disruption of the normal tau–tubulin interaction.[15] MTC has been used clinically since Paul Ehrlich first reported its use as an analgesic and in the treatment of malaria over a century ago.[49] Its main therapeutic use has been in the intravenous treatment of methaemoglobinaemia[50] and as an oral urinary antiseptic. It has also had clinical use in CNS, where it has been used to treat ifosfamide encephalopathy[51] and manic depression and psychosis.[52] MTC is not only a tau-aggregation inhibitor *in vitro*, but a compound that crosses the blood/brain barrier and demonstrates efficacy in reducing tau pathology and in relieving cognitive and motor learning symptoms in tau transgenic mice.

Furthermore, the rationale for using the TAI therapeutic approach has been confirmed by the results from a phase 2 clinical trial in 321 patients diagnosed with mild or moderate AD.[53] MTC reduced the rate of disease progression by 84% over 50 weeks when measured by the ADAS-cog scale and a 100% reduction on the MMSE scale, the two most common means to evaluate the usefulness of AD therapeutics. This result is a marked increase over the 30–50% reduction defined as desirable for an AD disease modifying agent by a European Task Force Consensus Statement.[54] These results were further supported by brain scans that allowed the visualisation of MTC-related prevention of loss of neuronal function as shown by a HMPAO-SPECT scan in a 55% subpopulation of the primary clinical study.[55] The accumulated data suggests that MTC has the potential not only to slow the rate of AD progression, but may even halt it and restore neuronal function, particularly at early stages of the disease.

References

1. A. Alzheimer, *Allg. Z. Psych. Psych.-gerich. Med.*, 1907, **64**, 146–148.
2. R. A. Crowther and C. M. Wischik, *EMBO J.*, 1985, **4**, 3661–3665.
3. C. M. Wischik, R. A. Crowther, M. Stewart and M. Roth, *J. Cell Biol.*, 1985, **100**, 1905–1912.
4. C. M. Wischik and R. A. Crowther, *Br. Med. Bull.*, 1986, **42**, 51–56.
5. C. M. Wischik, M. Novak, H. C. Thøgersen, P. C. Edwards, M. J. Runswick, R. Jakes, J. E. Walker, C. Milstein, R. M. and A. Klug, *Proc. Natl. Acad. Sci. USA*, 1988, **85**, 4506–4510.
6. C. M. Wischik, M. Novak, P. C. Edwards, A. Klug, W. Tichelaar and R. A. Crowther, *Proc. Natl. Acad. Sci. USA*, 1988, **85**, 4884–4888.

7. F. García-Sierra, C. M. Wischik, C. R. Harrington, J. Luna-Muñoz and R. Mena, *J. Chem. Neuroanat.*, 2001, **22**, 65–77.
8. E. B. Mukaetova-Ladinska, F. Garcia-Sierra, J. Hurt, H. J. Gertz, J. H. Xuereb, R. Hills, C. Brayne, F. A. Huppert, E. S. Paykel, M. McGee, R. Jakes, W. G. Honer, C. R. Harrington and C. M. Wischik, *Am. J. Pathol.*, 2000, **157**, 623–636.
9. C. R. Harrington, E. B. Mukaetova-Ladinska, R. Hills, P. C. Edwards, E. Montejo de Garcini, M. Novak and C. M. Wischik, *Proc. Natl. Acad. Sci. USA*, 1991, **88**, 5842–5846.
10. N. Zilka, P. Filipcik, P. Koson, L. Fialova, R. Skrabana, M. Zilkova, G. Rolkova, E. Kontsekova and M. Novak, *FEBS Lett.*, 2006, **580**, 3582–3588.
11. M. von Bergen, S. Barghorn, L. Li, A. Marx, J. Biernat, E. M. Mandelkow and E. Mandelkow, *J. Biol. Chem.*, 2001, **276**, 48165–48174.
12. T. C. Gamblin, M. E. King, H. Dawson, M. P. Vitek, J. Kuret, R. W. Berry and L. I. Binder, *Biochemistry*, 2000, **39**, 6136–6144.
13. E. Grober, D. Dickson, M. J. Sliwinski, H. Buschke, M. Katz, H. Crystal and R. B. Lipton, *Neurobiol. Aging*, 1999, **20**, 573–579.
14. D. R. Thal, T. Arendt, G. Waldmann, M. Holzer, D. Zedlick, U. Rüb and R. Schober, *Neurobiol. Aging*, 1998, **19**, 517–525.
15. C. M. Wischik, P. C. Edwards, R. Y. K. Lai, M. Roth and C. R. Harrington, *Proc. Natl. Acad. Sci. USA*, 1996, **93**, 11213–11218.
16. T. Nishimura, K. Hashikawa, H. Fukuyama, T. Kubota, S. Kitamura, H. Matsuda, H. Hanyu, H. Nabatame, N. Oku, H. Tanabe, Y. Kuwabara, S. Jinnouchi and A. Kubo, *Ann. Nuc. Med.*, 2007, **21**, 15–23.
17. M. F. Folstein, S. E. Folstein and P. R. McHugh, *J. Psychiatr. Res.*, 1975, **12**, 189–198.
18. H. Braak and E. Braak, *Acta Neuropathol.*, 1991, **82**, 239–259.
19. G. K. Wilcock and M. M. Esiri, *J. Neurol. Sci.*, 1982, **56**, 407–417.
20. C. R. Harrington, J. Louwagie, R. Rossau, E. Vanmechelen, R. H. Perry, E. K. Perry, J. H. Xuereb, M. Roth and C. M. Wischik, *Am. J. Pathol.*, 1994, **145**, 1472–1484.
21. H. Crystal, D. Dickson, P. Fuld, D. Masur, R. Scott, M. Mehler, J. Masdew, C. Kwas, M. Aronson and L. Wolfson, *Neurology*, 1988, **38**, 1682–1687.
22. P. W. Arriagada, J. H. Growdon, E. T. Hedley-White and B. T. Hyman, *Neurology*, 1992, **42**, 631–639.
23. T. G. Ohm, H. Müller, H. Braak and J. Bohl, *Neuroscience*, 1995, **64**, 209–217.
24. C. M. Wischik, D. Horsley, J. E. Rickard and C. R. Harrington, *PCT International Application*, 2002, WO02/055720.
25. B. Frost, R. L. Jacks and M. I. Diamond, *J. Biol. Chem.*, 2009, **284**, 12845–12852.
26. F. Clavaguera, T. Bolmont, R. A. Crowther, D. Abramowski, S. Frank, A. Probst, G. Fraser, A. K. Stalder, M. Beibel, M. Staufenbiel, M. Jucker, M. Goedert and M. Tolnay, *Nature Cell Biol.*, 2009, **11**, 909–914.

27. R. Y. K. Lai, H.-J. Gertz, D. J. Wischik, J. H. Xuereb, E. B. Mukaetova-Ladinska, C. R. Harrington, P. C. Edwards, R. Mena, E. S. Paykel, C. Brayne, F. A. Huppert, M. Roth and C. M. Wischik, *Neurobiol. Aging*, 1995, **16**, 433–445.
28. C. M. Wischik, R. Y. K. Lai and C. R. Harrington, in *Microtubule-Associated Proteins: Modifications in Disease*., ed. J. Avila, R. Brandt and K. S. Kosik, Harwood Academic Publishers, Amsterdam, Editon edn., 1997, pp. 185–241.
29. S. Love, L. R. Bridges and C. P. Case, *Brain*, 1995, **118**, 119–129.
30. K. Ohmi, L. C. Kudo, S. Ryazantsev, H.-Z. Zhao, S. L. Karsten and E. F. Neufeld, *Proceedings of the National Academy of Sciences*, 2009, **106**, 8332–8337.
31. D. N. Palmer, R. D. Martinus, S. M. Cooper, G. G. Midwinter, J. C. Reid and R. D. Jolly, *J. Biol. Chem*., 1989, **264**, 5736–5740.
32. R. A. Nixon and A. M. Cataldo, *Trends Neurosci*., 1995, **18**, 489–496.
33. E. D. Roberson, K. Scearce-Levie, J. J. Palop, F. Yan, I. H. Cheng, T. Wu, H. Gerstein, G.-Q. Yu and L. Mucke, *Science*, 2007, **316**, 750–754.
34. C. M. Wischik, J. E. Rickard, D. Horsley, C. R. Harrington, F. Theuring, K. Stamer and C. Zabke, *PCT International Application*, 2002, WO02/059150.
35. G. Chen, K. S. Chen, J. Knox, J. Inglis, A. Bernard, S. J. Martin, A. Justice, L. McConlogue, D. Games, S. B. Freedman and R. G. M. Morris, *Nature*, 2000, **408**, 975–979.
36. S. Perreault, O. Bousquet, M. Lauzon, J. Paiement and N. Leclerc, *J. Neuropathol. Exptl. Neurol*., 2009, **68**, 503–514.
37. O. Bugiani, J. R. Murrell, G. Giaccone, M. Hasegawa, G. Ghigo, M. Tabaton, M. Morbin, A. Primavera, F. Carella, C. Solaro, M. Grisoli, M. Savoiardo, M. G. Spillantini, F. Tagliavini, M. Goedert and B. Ghetti, *J. Neuropathol. Exptl. Neurol*., 1999, **58**, 667–677.
38. B. Allen, E. Ingram, M. Takao, M. J. Smith, R. Jakes, K. Virdee, H. Yoshida, M. Holzer, M. Craxton, P. C. Emson, C. Atzori, A. Migheli, R. A. Crowther, B. Ghetti, M. G. Spillantini and M. Goedert, *J. Neurosci*., 2002, **22**, 9340–9351.
39. J. Götz, F. Chen, R. Barmettler and R. M. Nitsch, *J. Biol. Chem*., 2001, **276**, 529–534.
40. J. Lewis, E. McGowan, J. Rockwood, H. Melrose, P. Nacharaju, M. Van Slegtenhorst, K. Gwinn-Hardy, M. P. Murphy, M. Baker, X. Yu, K. Duff, J. Hardy, A. Corral, W.-L. Lin, S.-H. Yen, D. Dickson, P. Davies and M. Hutton, *Nature Genet*., 2000, **25**, 402–405.
41. N. S. Honson, J. R. Jensen, A. Abraha, G. F. Hall and J. Kuret, *Neurotox. Res*., 2009, **15**, 274–283.
42. G. F. Hall, S. Lee and J. Yao, *J. Mol. Neurosci*., 2002, **19**, 253–260.
43. M. Pickhardt, Z. Gazova, M. von Bergen, I. Khlistunova, Y. Wang, A. Hascher, E.-M. Mandelkow, J. Biernat and E. Mandelkow, *J. Biol. Chem*., 2005, **280**, 3628–3635.
44. A. Crowe, C. Ballatore, E. Hyde, J. Q. Trojanowski and V. M. Y. Lee, *Biochem. Biophys. Res. Commun*., 2007, **358**, 1–6.

45. M. Pickhardt, G. Larbig, I. Khlistunova, A. Coksezen, B. Meyer, E. M. Mandelkow, B. Schmidt and E. Mandelkow, *Biochemistry*, 2007, **46**, 10016–10023.
46. S. Taniguchi, N. Suzuki, M. Masuda, S.-i. Hisanaga, T. Iwatsubo, M. Goedert and M. Hasegawa, *J. Biol. Chem.*, 2005, **280**, 7614–7623.
47. C. Chirita, M. Necula and J. Kuret, *Biochemistry*, 2004, **43**, 2879–2887.
48. A. Crowe, W. Huang, C. Ballatore, R. L. Johnson, A.-M. L. Hogan, R. Huang, J. Wichtermann, J. McCoy, D. M. Huryn, D. S. Auld, I. I. I. A. B. Smith, J. Inglese, J. Q. Trojanowski, C. P. Austin, K. R. Brunden and V. M. Y. Lee, *Biochemistry*, 2009, [Advance publication: http://dx.doi.org/10.1021/bi9006435].
49. J. E. Kristiansen, *Dan. Med. Bull.*, 1989, **36**, 178–185.
50. A. Mansouri and A. A. Lurie, *Am. J. Hematol.*, 1993, **42**, 7–12.
51. A. Kupfer, C. Aeschlimann, B. Wermuth and T. Cerny, *Lancet*, 1994, **343**, 763–764.
52. G. J. Naylor, B. Martin, S. E. Hopwood and Y. Watson, *Biol. Psychiatry*, 1986, **21**, 915–920.
53. C. M. Wischik, P. Bentham, D. J. Wischik and K. M. Seng, *Alzheimer's and Dementia*, 2008, **4**, T167.
54. B. Vellas, S. Andrieu, C. Sampaio, N. Coley and G. Wilcock, *Lancet Neurol.*, 2008, **7**, 436–450.
55. R. T. Staff, T. S. Ahearn, A. D. Murray, P. Bentham, K. M. Seng and C. Wischik, *Alzheimer's and Dementia*, 2008, **4**, T775.